

1 **Supplementary Information**

2

3 Phase transition behaviors and formation of electrically resistive  
4 phases at the anodes: Major factors determining the energy  
5 efficiency of Li-ion batteries

6 *Yong-Seok Choi and Jae-Chul Lee\**

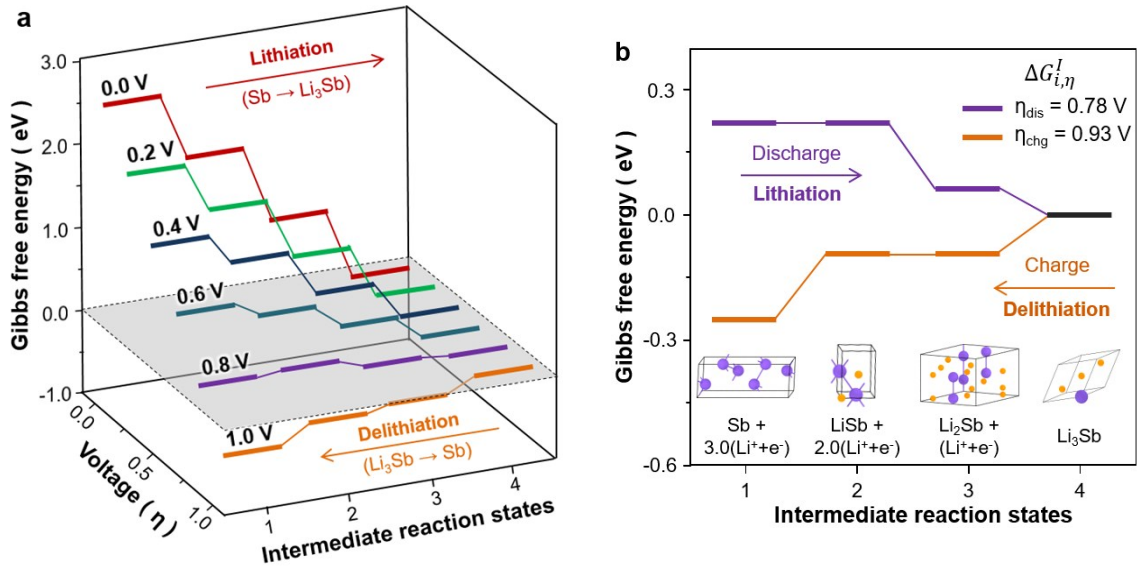
7 *Department of Materials Science and Engineering, Korea University, Seoul 02841, South Korea*

8 *\*To whom correspond should be addressed, E-mail: [jcleee001@korea.ac.kr](mailto:jcleee001@korea.ac.kr)*

9

10

11 **1. Calculation of the voltage values via Gibbs free energy curves for the Li–Sb battery.**



12

13 **Figure S1.** (a) Changes in the Gibbs free energy ( $\Delta G_{i,\eta}^I$ ) calculated for the intermediate reactions  
 14 occurring during Stage I transition ( $\text{Sb} \leftrightarrow \text{Li}_3\text{Sb}$ ) of the Li–Sb battery under various external voltages.  
 15 1, 2, 3 and 4 indicated on the  $x$ -axis denote the intermediate states corresponding to 3.0Li + Sb, 2.0Li  
 16 + LiSb, Li + Li<sub>2</sub>Sb and Li<sub>3</sub>Sb, respectively. (b) Representative graphs selected from (a), showing the  
 17 changes in the Gibbs free energy of the intermediate reactions at the critical voltages corresponding  
 18 to the discharge ( $\eta_{\text{dis}}$ ) and charge ( $\eta_{\text{chg}}$ ) in Stage I transition. The structures in the inset of (b) are four  
 19  $\text{Li}_x\text{Sb}$  phases formed by the intermediate reactions in the Li–Sb battery. In these structures, Li and Sb  
 20 atoms are distinguished by yellow and purple spheres, respectively.

21

22 During the charge and discharge processes, the Li–Sb system undergoes a single phase transition  
 23 corresponding to  $\text{Sb} \leftrightarrow \text{Li}_3\text{Sb}$ , which is referred to as the Stage I transition. In order to replicate the  
 24 voltage curves associated with the battery cycles at the Sb anode of the Li–Sb system, it is therefore

25 necessary to evaluate the discharge ( $\eta_{\text{dis}}$ ) and charge voltages ( $\eta_{\text{chg}}$ ) corresponding to the Stage I  
 26 transition. In this section, using procedures similar to those discussed in Fig. 5 of the manuscript, we  
 27 evaluated the  $\eta_{\text{dis}}$  and  $\eta_{\text{chg}}$  values by calculating the changes in the Gibbs free energy of the  
 28 intermediate reactions in the Stage I transition of the Li–Sb battery. For this purpose, we first  
 29 evaluated the Gibbs free energy change ( $\Delta G_i^I$ ) associated with the  $i^{\text{th}}$  intermediate reaction in Stage I  
 30 transition. This was achieved by using the Gibbs free energies of all phases (Li, Sb, and  $\text{Li}_x\text{Sb}$  phases)  
 31 comprising the  $i^{\text{th}}$  intermediate reaction state according to:

$$32 \quad (\text{Stage I transition}) \quad \Delta G_{i,\eta}^I = 3G_{\text{Li}} + G_{\text{Sb}}, i = 1. \quad (\text{S1.1})$$

$$33 \quad \Delta G_i^I = (3 - x)G_{\text{Li}} + xG_{\text{Li}_x\text{Sb}}, i = 2, 3, 4. \quad (\text{S1.2})$$

34 When the external voltage/potential  $\eta$  is imposed on the Li–Sb system, the Gibbs free energy of  
 35 each intermediate reaction in Eq. (S1) decreases further in proportion to the number of Li atoms that  
 36 do not participate in the reaction forming the lithiated compound of  $\text{Li}_x\text{Sb}$ , i.e.,  $(3 - x)$ . Therefore,  
 37 under external voltages imposed to the system, the Gibbs free energy of each intermediate state in  
 38 Stage I transition can be evaluated as:

$$39 \quad (\text{Stage I transition}) \quad \Delta G_{i,\eta}^I = 0.5G_{\text{Li}} + G_{\text{Sb}} - (3.0 - x)\eta, i = 1. \quad (\text{S2.1})$$

$$40 \quad \Delta G_{i,\eta}^I = (3.0 - x)G_{\text{Li}} + xG_{\text{Li}_x\text{Sb}} - (3.0 - x)\eta, i = 2, 3, 4. \quad (\text{S2.2})$$

41 As shown in Eq. (S2), the external voltage ( $\eta$ ) changes the Gibbs free energies ( $\Delta G_{i,\eta}^I$ ) of each  $i^{\text{th}}$   
 42 intermediate reaction state in Stage I and thus, alters the overall shape of the Gibbs free energy curve  
 43 during charging and discharging. According to the definitions in the manuscript, the  $\eta_{\text{dis}}$  value is the

44 highest voltage at which all intermediate reactions are in the free-energy downhill in the direction of  
 45 the discharge process (i.e.,  $3.0\text{Li} + \text{Sb} \rightarrow \text{Li}_3\text{Sb}$ ), whereas the  $\eta_{\text{chg}}$  value is the lowest voltage at which  
 46 all intermediate reactions are in the free-energy downhill in the direction of the charge process (i.e.,  
 47  $\text{Li}_3\text{Sb} \rightarrow 3.0\text{Li} + \text{Sb}$ ). By substituting the various  $\eta$  values, we obtained the  $\eta_{\text{dis}}$  and  $\eta_{\text{chg}}$  values  
 48 satisfying the above-mentioned criteria (Fig. S1). The calculated values of the  $\eta_{\text{dis}}$  and  $\eta_{\text{chg}}$   
 49 corresponding to the Stage I transition are 0.78 and 0.93 V, respectively, and are summarized in Table  
 50 3 in the manuscript.

51

## 52 2. Predicted intermediate phases of Li–Sb and Li–Si battery.

53 **Table S1.** Predicted  $\text{Li}_x\text{Sb}$  phases formed during the battery cycle predicted by the current and  
 54 previous works <sup>S1</sup>. The phases predicted by atomic simulations (○) and those identified by both  
 55 theory and experiments (●) are distinguished by different symbols.

Space group of predicted structures	x of $\text{Li}_x\text{Sb}$									
	Stage I (Sb ↔ $\text{Li}_3\text{Sb}$ )									
	0	0.33	0.43	0.5	0.6	1	2	2.7	3	
$\text{Fm}\bar{3}\text{m}$							○		○	
$\text{P6}_3/\text{mmc}$									○	
$\text{R}\bar{3}\text{m}$	●									
$\text{C2}/\text{m}$								○		
$\text{Im}\bar{3}\text{m}$		○	○	○	○	○	○			●

57

58 **Table S2.** Predicted  $\text{Li}_x\text{Si}$  phases formed during the battery cycle predicted by present and previous  
 59 works <sup>S1,2</sup>. Among these phases, the phases predicted by atomic simulations (○) and those identified  
 60 by both theory and experiments (●) are distinguished by different symbols.

Space group of predicted structures	x of $\text{Li}_x\text{Si}$									
	Stage I ( $\text{Si} \leftrightarrow \text{Li}_{3.75}\text{Si}$ )									
	0	0.33	1	1.71	2	Stage II ( $\text{Li}_{2.33}\text{Si} \leftrightarrow \text{Li}_{3.75}\text{Si}$ )				
					2.33	3.25	3.5	3.75		
$\text{Fd}\bar{3}\text{m}$	●									
$\text{P6}_3/\text{mmc}$		○						○		
$\text{R}\bar{3}\text{m}$					○					
$\text{I}\bar{4}3\text{d}$										●
$\text{I4}_1/\text{a}$			○	○						
$\text{Pnma}$				○						
$\text{Pbam}$								○	○	
$\text{P3}_212$						○				
$\text{P}\bar{3}\text{m1}$						○				

61

62

63

## REFERENCES

- (S1) Belsky, A.; Hellenbrandt, M.; Karen, V. L.; Luksch, P., New Developments in the Inorganic Crystal Structure Database (Icsd): Accessibility in Support of Materials Research and Design. *Acta Crystallographica Section B: Structural Science* **2002**, *58* (3), 364-369.
- (S2) Braga, M. H.; Dębski, A.; Gąsior, W., Li–Si Phase Diagram: Enthalpy of Mixing, Thermodynamic Stability, and Coherent Assessment. *J. Alloys Compd.* **2014**, *616*, 581-593.